DETECTION AND SEGMENTATION OF POLE-LIKE OBJECTS IN MOBILE LASER SCANNING POINT CLOUDS

A. Nurunnabi[1,2*], Y. Sadahiro[3], F. N. Teferle[1,2], D. F. Laefer[4], J. Li[5]

[1] Geodesy and Geospatial Engineering, Faculty of Science, Technology and Medicine, University of Luxembourg
6, rue Richard Coudenhove-Kalergi, L-1359 Luxembourg − (abdul.nurunnabi, norman.teferle)@uni.lu
[2] Institute for Advanced Studies (IAS), University of Luxembourg, Luxembourg
[3] Interfaculty Initiative in Information Studies, The University of Tokyo, Japan − sada@csis.u-tokyo.ac.jp
[4] Center for Urban Science and Progress and Department of Civil and Urban Engineering, Tandon School of Engineering, New York University, 370 Jay St., #1301C, Brooklyn, NY 11201 USA − debra.laefer@nyu.edu
[5] Geography and Environmental Management, University of Waterloo, Waterloo ON N2L 3G1, Canada − junli@uwaterloo.ca

KEY WORDS: City Modelling, Intelligent Transportation, Saliency Feature, Mobile Mapping, Road Safety, Robust Statistics

ABSTRACT:

Pole-like object (PLO) detection and segmentation are important in many applications, such as 3D city modelling, urban planning, road assets monitoring, intelligent transportation, road safety, and forest monitoring. Arguably, vehicle-based mobile laser scanning (MLS) is the best on-road data acquisition system, because it is fast, precise and non-invasive. As part of that, laser scanning georeferenced data (i.e., point clouds) provide detailed structural morphology of the scanned objects. However, point clouds are not free from outliers and noise. Critically, many of the object extraction methods that depend on local saliency features (e.g., normals)-based segmentation use principal component analysis (PCA). PCA can provide the local features but struggle to produce robust results in the presence of outliers and noise. To reduce the influence of outliers for saliency features estimation and in segmentation, this paper employs Robust distance-based Diagnostic PCA (RD-PCA) coupled with the well-known DBSCAN clustering algorithm. This study contributes to a better understanding of object detection and segmentation by (i) exploring the problems of local saliency features estimation in the presence of outliers and noise; (ii) understanding problems with PCA and why RD-PCA is important; and (iii) introducing a novel method for PLOs detection and segmentation following a robust segmentation approach. The performance of the new algorithm is demonstrated through MLS data acquired in an urban road setup.

1. INTRODUCTION

There are many types of objects in urban road environments, including buildings, trees, cars and poles. This paper focuses on pole-like objects (PLOs). Detection, delineation and segmentation of PLOs located in a road environment have great importance in roadway inventory (Chen et al., 2022), high density (HD) map generation (Plachetka et al., 2021), city modelling, urban planning, road infrastructure monitoring (Ha and Chaisomphob, 2020), intelligent transportation (Wang et al., 2021; Nurunnabi et al., 2022), traffic management (Tang et al., 2020; Li &Cheng., 2022), and most highly road safety inspection applications, as well as averting roadside accidents (Cabo et al., 2014; Wang et al., 2021). Image and video data are common to use for PLOs detection (Zhang et al., 2018; Sheweta et al, 2022). While two-dimensional (2D) drawings of road furniture may be available, three-dimensional (3D) interpretation and advanced analysis (Yadov et al., 2022) is not readily achieved.

An alternative is Light Detection and Ranging (LiDAR) technology, which integrates laser scanners, global navigation satellite systems (GNSS) and inertial measurement units (IMU) to provide 3D (*x, y,* and *z*; a trio) georeferenced data known as point clouds. Point cloud provide detailed 3D geometry and spatial information of the scanned objects' structure. In mobile laser scanning (MLS) systems, the scanning sensors are mounted on a vehicle, GNSS and IMU systems are also on board. Vehicle-based MLS systems are fast, precise, non-invasive and, thus, reduce hugely manual labour requirements (Lehtomaki et al., 2015). These point clouds contain a large number of points calls for the efficiency of precise mapping of various roadway features. Although point clouds can provide more facilities to extract geometric detail rather than imagery, processing point clouds is extra challenging, because the data are unordered, typically partial, locally sparse, have irregular point density and do not follow any statistical distribution. Moreover, point clouds are not free from outliers and noise (Nurunnabi et al., 2015; 2019). Critically, the outliers rarely have a pattern or distribution (Nurunnabi et al., 2014a) and frequently occur because of line-of-sight obstruction and multiple reflectance (Sotoodeh, 2006). The presence of outliers can negatively impact normal and curvature estimation accuracy. The reader is referred to Nurunnabi et al. (2012, 2015, 2016b) to know further about the issues of outliers and noise in point cloud processing (e.g., saliency features estimation and segmentation).

A multitude of methods have been proposed for PLOs detection and extraction over the years. Existing methods can be grouped into four major categories based on the techniques/principles employed: (i) slicing, (ii) voxelization, (iii) classification or segmentation, and (iv) model fitting. An early slicing technique was developed by Luo and Wang et al. (2008) for PLOs. In that the point cloud is sliced into multiple sections and then "pillars" are detected by projective parameters. Subsequently, Yu et al. (2015) developed a voxel-based method in which ground points are removed using a voxel-based upward growing approach. Next, non-ground points were segmented and clustered using voxels and normalized cut segmentation. A hierarchical classification approach to delineate PLOs was introduced by Liu et al. (2020). In that the PLOs were extracted using eigenvalues and data directions. Critically, this method has proved unsuitable when the data are sparse and outliers are present (Wang et al., 2021). Recently, Tang et al. (2020) coupled a Euclidean distance-based clustering with a minimum cut method to

*Corresponding author

segment the road scene, and combined it with support vector machines (Cortes & Vapnik, 1995) to segment and classification of pole-like traffic facilities. A lot of work has been done in fitting, with RANSAC (Fischler and Bolles, 1981) as the heart of many algorithms (Tarsha-Kurdi et al., 2008). Golovinskiy et al. (2009) developed a four-step method: locating, segmenting, characterizing, and classifying clusters of 3D points. RANSAC-is useful to get planar patches to remove ground points, and then uses classification methods to get PLOs (Tombari et al., 2014). In recent years, deep learning (DL) approaches have been used in PLOs detection and extraction (Fang et al., 2022; Sheweta et al., 2022). Plachetka et al. (2021) developed a PLOs recognition algorithm with an end-to-end deep neural network (DNN)-based approach using high-density LiDAR point clouds. This method learns an optimal feature representation for various, principally generic, classes of poles in an end-to-end fashion.

There are many hybrid methods available in the literature that use different tasks to get better results. For example, Wang et al. (2021) proposed a PLOs segmentation method under geometric structural constraints. In that, first the data were voxelized excluding the ground points. Then the rod-shaped parts were extracted according to the vertical continuity. Next, a regional growth was performed based on the voxels to retain the non-rod parts. Finally, a random forest (RF; Breiman, 2001) model was employed to classify the PLOs using local and global features. Unfortunately, most of the existing methods have the problems of partial extraction of PLOs and the insufficient recognition accuracy (Wang et al., 2021). Nevertheless, the identification of PLOs remains a complex and challenging task as poles on the roadways have different shapes and sizes, and frequently come with a variety of complex attachments (e.g., signposts, traffic signs, traffic lights, or lamps). Because of the characteristic thin shape of PLOs, detection is negatively impacted by both noise as well as occlusions and clutter (Tombari et al., 2014). Thus, existing methods are still not sufficient for robust and precise results with real world datasets. Today, many of the object extraction methods that depend on local saliency features (e.g., point normals and curvature)-based segmentation (Lalonde et al., 2006) use principal component analysis (PCA). PCA can provide the local features, but it is evident that PCA-based features are unreliable and non-robust in the presence of outliers and noise (Nurunnabi et al., 2012; 2015). To reduce the influence of outliers for saliency features estimation, clustering and segmentation, this paper employs Robust distance based Diagnostic PCA (RD-PCA; based on MCMD-Z) introduced in (Nurunnabi et al., 2015), and the well-known density-based spatial clustering of applications with noise (DBSCAN) algorithm (Ester et al., 1996). This paper introduces a novel algorithm that combines DL for ground surface removing, spatial clustering for object isolation, DBSCAN to get vertical parts, and RD-PCA for region-growing-based segmentation to extract PLOs. Scientific contributions of this paper are as follows: (i) a novel algorithm is proposed that detects and extracts PLOs in a road environment, (ii) exploration of problems of local saliency feature estimation in the presence of outliers, (iii) demonstration of how PCA is influenced by outliers, including why RD-PCA is important, and how it produces robust results, and (iv) validation of the new algorithm with respect to producing robust results in the presence of outliers and/or noise. The performance of the algorithm is demonstrated through MLS point clouds.

The remaining paper is presented as: Section 2 briefly presents the basic principles and methods used in the proposed algorithm. Section 3 proposes the methodology of the new algorithm. Section 4 demonstrates the new algorithm using two real-world MLS datasets. Section 5 concludes the paper.

2. RELATED PRINCIPLES AND METHODS

This section presents a short discussion of related methods and principles that are used in the proposed algorithm in Section 3.

2.1 Existing methods for ground surface extraction

Precise ground surface point extraction and removal them from the on-ground objects is important for PLOs extraction, as it greatly simplifies the remainder of work, in part by reducing the size of the dataset, thus dropping the computational burden. Vosselman (2000) developed an algorithm based on mathematical morphology, a slope-based approach for ground points extraction. Nurunnabi et al. (2016a) proposed a segment-based approach using robust locally weighted regression to remove the ground points. There are many more methods exist in the literature including the well-known surface-based (Kraus and Pfeifer, 1998) and progressive densification-based (Axelsson, 2000) approaches. Recently, DL-based methods are frequently applied.

Nurunnabi et al. (2021) introduced a feature-based DL method for ground and non-ground points isolation. This method has the advantage that does not require transformation of point clouds into raster image or any voxel-based regular 3D grids that are susceptible to information loss (Qi et al., 2017). The algorithm has two primary steps: (i) the first consists of relevant features extraction and finding optimum feature space, and (ii) the second develops a DL-based binary classifier that classifies points into ground and non-ground points. The approach is based on the features (e.g., points' local neighborhood-based covariance features, such as linearity, planarity and point normals) that have been frequently used for classification and semantic segmentation in point clouds. These local saliency features can be estimated using Robust distance-based Diagnostic PCA (RD-PCA; Nurunnabi et al., 2015). A brief discussion about RD-PCA is provided in Section 2.3. The feature-based DL algorithm is a shallow network follows a basic structure of a neural network. The network used rectified linear unit (ReLU) activation function for the internal layers, and a Sigmoid function for the output layer, where the well-known binary cross entropy is used as the loss function with the ADAM optimizer to speed up the training process. The reader is referred to (Nurunnabi et al., 2021) to know detail about the algorithm.

2.2 DBSCAN

DBSCAN is a non-parametric approach (Ester et al., 1996) and one of the most frequently applied clustering algorithms. This density-based algorithm groups closely located points in a space and marks those further away as outliers that typically lie alone or scattered in low-density regions. Two main parameters ε (the distance that defines the neighborhood, i.e., maximum distance between the point of interest and its neighbors) and MinPTS (least number of points to define a density threshold for a cluster) are necessary to implement DBSCAN. DBSCAN starts by selecting a random point p_i from a dataset and allocate it to a cluster C_1. Then it counts the number of points (n) within the ε distance from p_i, if $n \geq$ MinPTS then p_i is considered as a core point, then it will insert all these neighbors to the same cluster C_1. Afterwards, each point of cluster C_1 finds their respective neighbors with the ε distance. If a point in the cluster C_1 has n or more neighbors within ε distance, it will be included in C_1. The approach continues to grow C_1, until there are no more points within its' reach. This process then considers another point from the dataset that does not belong to any cluster and puts it in cluster C_2. This continues until all points are exhausted. Unlike

the *k*-means clustering, DBSCAN does not require pre-specifying the number of clusters and tends to be more reliable results. For example, it can find clusters of arbitrary shapes, and discovers a cluster completely surrounded by a different cluster without getting any connection (Fig. 1). However, it is highly sensitive to the values of ε and MinPTS, hence the user needs to have a clear understanding about the two parameters.

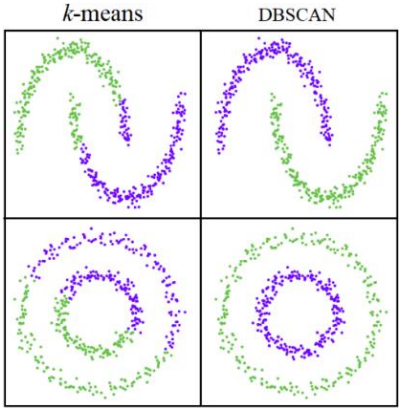

Figure 1. *k*-means and DBSCAN clustering results for two simulated datasets. *k*-means produces faulty results.

2.3 PCA and RD-PCA

PCA is a statistical technique, primarily was used for dimension reduction in a dataset. This has been extensively used for local saliency features estimation and point cloud processing. It is evident that PCA is sensitive to outliers, means that inaccurate in fitting plane parameters in the presence of outliers (Mitra et al., 2003; Nurunnabi et al., 2012). Nurunnabi et al. (2014b, 2015) showed that robust and diagnostic PCA can reduce the influence of outliers and produce robust saliency features. PCA transforms the original variables to a new set of uncorrelated-orthogonal variables, called principal components (PCs). PCs are the linear combination of the original variables that are arranged the variability in the data through the variance. A covariance matrix (Σ) of k points (neighbors) for a point of interest p_i in a point cloud P can be defined as:

$$\Sigma_{3\times3} = \frac{1}{k}\sum_{i=1}^{k}(p_i - \bar{p})\,(p_i - \bar{p})^T, \quad (1)$$

where $\bar{p} = \frac{1}{k}\sum_{i=1}^{k} p_i;\ p_i\,(x, y, z) \in P$, and $P \in R^3$. To perform PCA and to derive PCs, we solve the following eigenvalue equation by using the singular value decomposition technique,

$$\boldsymbol{\lambda} V = \Sigma V, \quad (2)$$

where V is a matrix of eigenvectors (PCs), $\boldsymbol{\lambda}$ is a diagonal matrix of three eigenvalues ($\lambda_2 \geq \lambda_1 \geq \lambda_0$). Besides, classical PCA there are variants of robust PCA [e.g., ROBPCA (Hubert et al., 2005)] produced robust PCs in the presence of outliers and noise. There are many alternatives. One by Nurunnabi et al. (2013; 2014b) follows principles of diagnostic statistics to find outliers and then uses classical PCA to the outlier free dataset.

Robust distance-based Diagnostic PCA (RD-PCA) was introduced in Nurunnabi et al. (2015) to find outliers in point cloud data and to estimate local saliency features (i.e., point normals and curvatures) without outlying data. RD-PCA follows the basic principle of diagnostic PCA, as a means for identifying outliers in a dataset and then performing PCA to the outlier free data. For a point cloud, when RD-PCA produces robust saliency features it finds outliers locally in a local neighborhood of a point of interest, and then makes a covariance matrix with inliers and find PCs by using classical PCA. The standard procedure of robust outlier detection is finding outliers by searching for the model fitted to the majority of the data, hence it needs to find the most consistent set (MCS) of points those are consistent to each other. The MCS set was found in a robust way. This algorithm assumes that points in a sufficiently small local neighborhood are on a planar surface. Two metrices: point to plane orthogonal distance (OD) and the surface points variation (the third eigenvalue) along the normal are estimated based on local neighbor points of an interest point used to find the outliers. Only a subset of h ($h = \lceil 0.5k \rceil$, and k is the number of points in a local neighborhood) points, the majority of good (inlier) points that are homogeneous and reliable, and have the minimum sorted ODs are used to fit the plane and calculates respective surface point variation.

In order to get the best set of h points, the algorithm begins with the minimal number of points, h_0 in case of plane fitting $h_0 = 3$. An outlier free h-subset can be found after a sufficient number of repetitions following the basic principle of RANSAC (Fischler and Bolles, 1981), and the h-subset then can produce better plane parameters. This h-subset is defined as the MCS. Now, a plane is fitted using the MCS set for the local neighborhood, and calculate the robust orthogonal distances (ODs) for all the points in the neighborhood using point mean ($\bar{p}$), and estimated normal ($\hat{n}$) using Eq. (3),

$$OD(p_i) = (p_i - \bar{p}).\hat{n}\,. \quad (3)$$

Finally, the robust Z (Rz_i) scores are calculated for the points in a local neighborhood,

$$Rz_i = \frac{[OD_i - median\ (OD_i)]}{MAD\ (OD_i)}, \quad (4)$$

and the points with Rz_i values more than 2.5 are considered as outliers. The reader is referred to Nurunnabi et al. (2015) for detail about RD-PCA.

3. METHODOLOGY

A six-step method for PLOs detection and extraction is proposed in this section (workflow is in Fig. 2).

Step 1. Ground surface points elimination
Laser scanning point clouds typically consist of both ground and non-ground points. As PLOs are on-ground objects; ground points are removed to reduce the data volume. The feature-based light-weight DL algorithm developed in Nurunnabi et al. (2021) is used for this task. The authors (Nurunnabi et al., 2021) proposed three Models (1, 2, 3) in their paper, we have considered the Model 3 as this is better than the others to filter out the ground points. That method has shown a 97% accuracy for classifying ground and non-ground points in large-scale outdoor point clouds including road scene. We select this method to reduce a significant amount of the computational complexity, and time when compared to typical end-to-end DL methods (e.g., Qi et al., 2017) in point cloud semantic segmentation.

Step 2. Spatial clustering
Here, on-ground objects are isolated as individual clusters using 3D Euclidean distance (ED)-based spatial clustering. Spatial clustering works as a region growing-based segmentation. It starts from a seed point having the lowest z value in the dataset then starts growing a region (group) with the points having ED less than a predefined threshold, ED_{th}. Each point in the group works as a subsequent seed point for continuing the group, until it finishes to accumulate a complete (or part of) object.

Figure 2. The pipeline of the proposed PLOs extraction method.

A region with more than a minimum number of points (M_p) is considered as an individual object. This process continues until all the points in the data are considered as a seed point.

Step 3. Identification of potential PLOs

PLOs are typically attached to the ground surface and have more than a minimum height and width. Hence, we search for the potential PLOs from the results of the spatial clustering is based on these three criteria: (i) being attached to or in close proximity (within a ground level threshold; $G_{th} = 0.5$) to the ground surface, (ii) having spatial extents in the *z*-direction exceeding 0.5m, and (iii) possessing horizontal extents (i.e., range of *x* or *y*) of less than 1m in its lower portion. However, since PLOs such as billboards or light-poles are often surrounded by other vegetation/bush, these can be wrongly included during the clustering.

Step 4. Extraction of the vertical part of a PLO

Next the DBSCAN clustering algorithm is applied to extract vertical parts of the potential PLOs. For this, the 3D (*x*, *y*, *z*) data is projected onto a 2D (*x*-*y* directions) plane. After density-based clustering, DBSCAN can identify most dense parts of an object. Projection of the 3D objects in 2D, results in a 2D point density in which the vertical part of a PLO is the densest. Resultant densest parts are the considered as vertical parts of the PLOs. Surrounding objects like leaves of trees can complicate this step.

Step 5. Improvement of vertical parts of PLOs

As mentioned in Section 2, PCA-based saliency features are influenced by outliers and noise but are aided by RD-PCA. Fig 3(a) shows how PCA based normals failed to discriminate two distinct surfaces near an edge of a road curb/boundary, whereas RD-PCA-based normals successfully identified them. In this algorithm RD-PCA is applied to get robust PCs and eigenvalues. Using RD-PCA based saliency features, segmentation is achieved following a conventional region growing approach and applying Eq. (5). This segmentation obtains precise vertical parts that are only with PLOs and correct errors from Step 4. Eq. (5) is defined as:

$$\left.\begin{array}{l}\text{(i) } \mathrm{N}_{z_i} < \mathrm{N}_{z_{th}}\,, \\ \text{(ii) } \theta_{ij} < \theta_{th}\,, \\ \text{(iii) } \mathrm{ED}_{ij} < \mathrm{ED}_{th}\end{array}\right\}, \tag{5}$$

where N_{z_i} (the value of the normal vector's z component) can be defined as:

$$\mathrm{N}_{z_i} = |\vartheta_0 \,.\, n_z\,|, \tag{6}$$

where ϑ_0 is the third eigenvector (i.e., normal), $n_z = (0, 0, 1)$; θ_{ij} and ED_{ij} is the angle between $\boldsymbol{p_i}$ and $\boldsymbol{p_j}$ (*j*th neighbor of $\boldsymbol{p_i}$) and ED is between $\boldsymbol{p_i}$ and $\boldsymbol{p_j}$, respectively. The terms $\mathrm{N}_{z_{th}}$, θ_{th} and ED_{th} are their respective thresholds. The value of the normal vector's z component can explain the local surface (that belongs to the point p_i) structure (i.e., vertical or horizontal) [as per Liang et al., 2012]. Fig. 3(a) shows how PCA based normals struggle with edge points, and the N_z values change over the surface position (horizontal or vertical). A point on a vertical surface reasonably has a significantly less value of N_z than a point on a horizontal surface, Fig. 3(b).

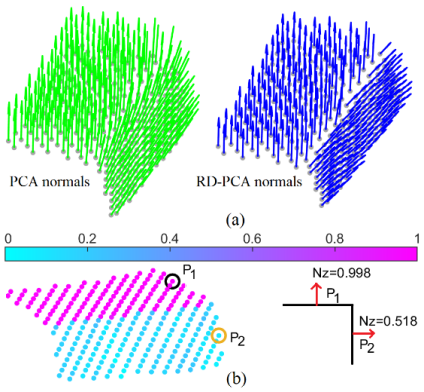

Figure 3. (a) PCA and RD-PCA based normals, PCA normals are not successful to discriminate between a horizontal and vertical surface near a road edge, but RD-PCA normals are successful, (b) N_z values for p_1 (on horizontal surface) and p_2 (on vertical surface) are significantly different.

Step 6. Removal of non-pole objects

For the removal of non-pole objects, the criteria of the points (within 1m) above the extracted vertical parts are investigated. The points' normal-based angle variation metric is employed to define points' linearity, planarity, or scatteredness to remove unwanted non-pole objects that may come from different objects surface, e.g., parts of trees. This metric is the standard deviation (SD) of θ_{ij} (angle between two points, Fig. 4), and SD (θ_{ij}) can be defined as:

$$\mathrm{SD}\left(\theta_{ij}\right) = \sqrt{\tfrac{1}{k}\textstyle\sum_{j=1}^{k}\left(\theta_{ij} - \bar{\theta}\right)^2}\,, \tag{7}$$

where, $\bar{\theta}$ is the mean of θ_{ij}; $j = 1, 2, \ldots, k$.

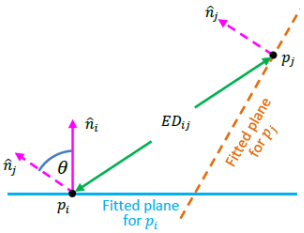

Figure 4. Angle (θ) between two points ($p_i,\ p_j$).

We consider, a point is planar/linear/scatter if it follows Eq. (8).

$$\left.\begin{array}{c} SD\left(\theta_{ij}\right) < 1^0; planar \\ 1^0 \le SD\left(\theta_{ij}\right) < 10^0; linear \\ 10^0 \le SD\left(\theta_{ij}\right); scatter \end{array}\right\}. \tag{8}$$

If majority (more than 80%) of the points are from a non-pole object, they are considered scatter. This way, trees (which have a pole-like structure, i.e., tree trunk) are avoided. Finally, complete objects that have all parts together with the vertical portion selected by RD-PCA segmentation and spatial clustering are declared as the extracted PLOs.

4. EXPERIMENTS, EVALUATION AND DISCUSSION

In this section, the proposed algorithm is demonstrated through experiments on a pair of vehicle-based MLS point cloud datasets.

4.1 Experiment 1

The first experiment was based on an MLS point cloud acquired in urban road site, Warringa, Australia. This dataset (Fig. 5a) covers a road scene along the roadway of 48m length with a total of 931,497 points. It has 17 PLOs, including 1 utility pole, 6 traffic signal-light poles, 7 sign poles, 1 long light pole, and 2 bollards, also gets many non-PLOs such as trees, buildings, and cars. The DL-based ground point filtering algorithm (Nurunnabi et al., 2021) was applied that separates ground surface (697, 252 points; gray) and non-ground objects (Fig. 5b). Then the ED-based clustering (with $ED_{th} = 0.1m, M_p = 50$) was performed on the remaining non-ground points. The results (Fig. 5c) are of individual objects or parts of objects (e.g., tree branches or leaves having irregular shapes and scattered). A total of 32 potential PLOs were obtained (Fig 5d) using the rule-based approach in Step 3. The DBSCAN-based clustering was performed to find the vertical portion of the PLOs. In Fig. 5e, a sign-plate attached to a sign pole (object 14) has found wrong as a vertical part. Fig. 5f explores DBSCAN results for a traffic-light pole [object 17, plot (i)], and the 2D and 3D cluster results are plotted in (Fig. 5f-ii) and (Fig. 5f-iii), respectively. The main vertical part (maroon) is clearly visible in Fig. 5f(iii). Next PCA and RD-PCA based segmentation was done to the DBSCAN results. Results are shown for objects 14 and 23 in Fig. 5g. These images illustrate the consequences of the presence of outliers and noise on PCA and RD-PCA based saliency features estimation (k=30), and consequently, on segmentation intended for vertical part identification. The PCA-based results for object 14, a sign plate attached to the sign pole, were incorrectly identified as a vertical part. For object 23, some of the non-vertical points (red) were identified as vertical points. The main cause was the smoothing which occurs with the PCA normals on edge-like surfaces.

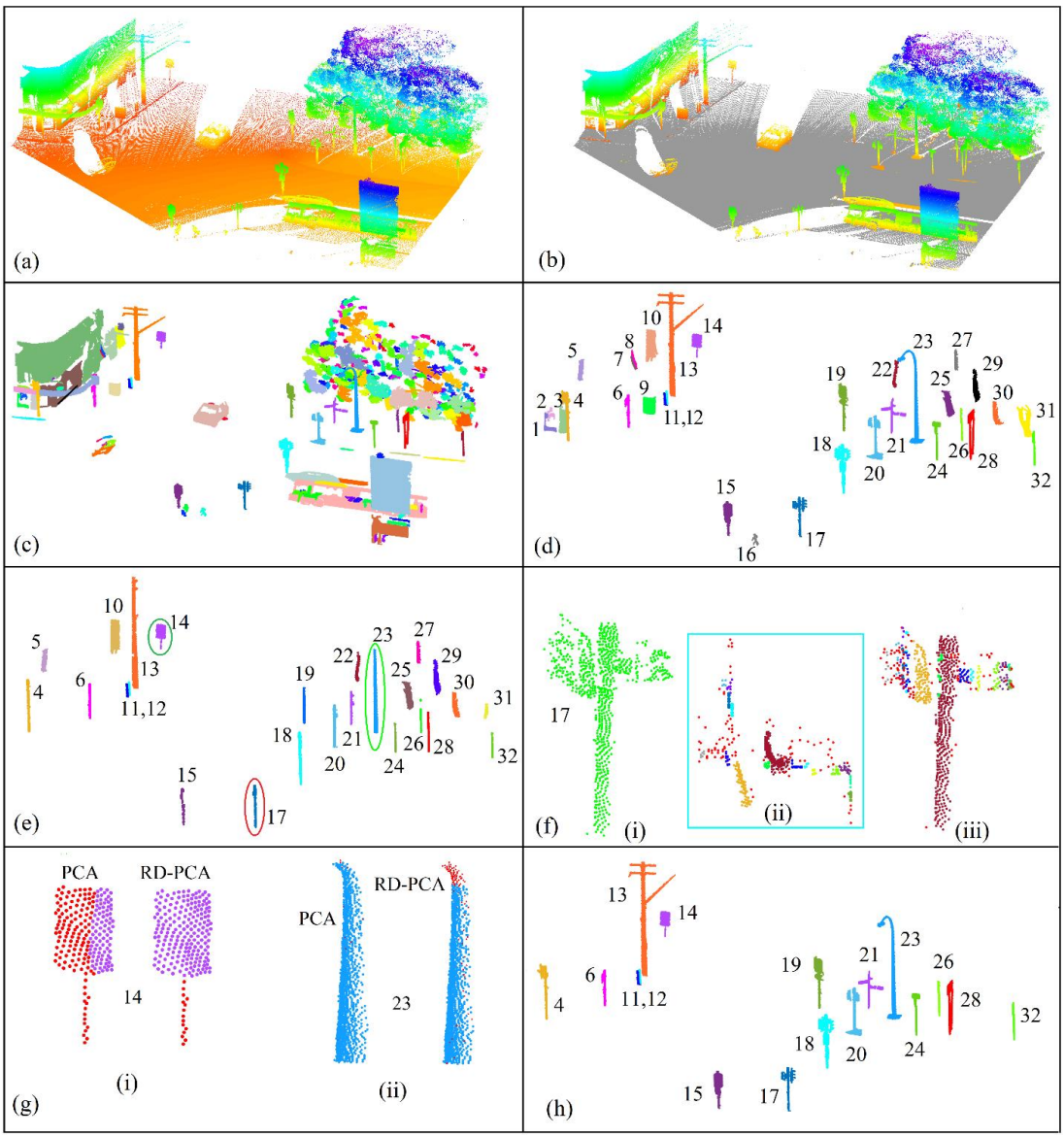

Figure 5. Pole-like objects (PLOs) extraction: (a) MLS point cloud of a road scene, (b) classification of ground and non-ground points, (c) results of ED-based spatial clustering, (d) potential PLOs, (e) DBSCAN results, detection of vertical parts, (f) (i) Object 17, a 3D traffic light pole, (ii) 2D projection results, (iii) detected 3D parts (color plot), vertical part is in maroon, (g) PCA and RD-PCA based segmentation results: (i) sign pole, and (ii) long light pole, (h) elimination of non-PLOs, and final extracted PLOs.

In contrast, the RD-PCA based normals successfully separated the planar and vertical surfaces. Linearity, planarity, and scatteredness were checked by applying Step 6. The rules in Eq. (8) were able to remove the scattered surface points that were mostly tree parts (e.g., objects 25, 29 and 30). Finally, all 17 PLOs were successfully extracted (Fig. 5h).

4.2. Experiment 2

This second experiment uses a portion of an open access MLS point cloud (Fig. 6a) from a road environment in Lille, France. This is an open access dataset, Paris-Lille-3D (Roynard et al., 2018).

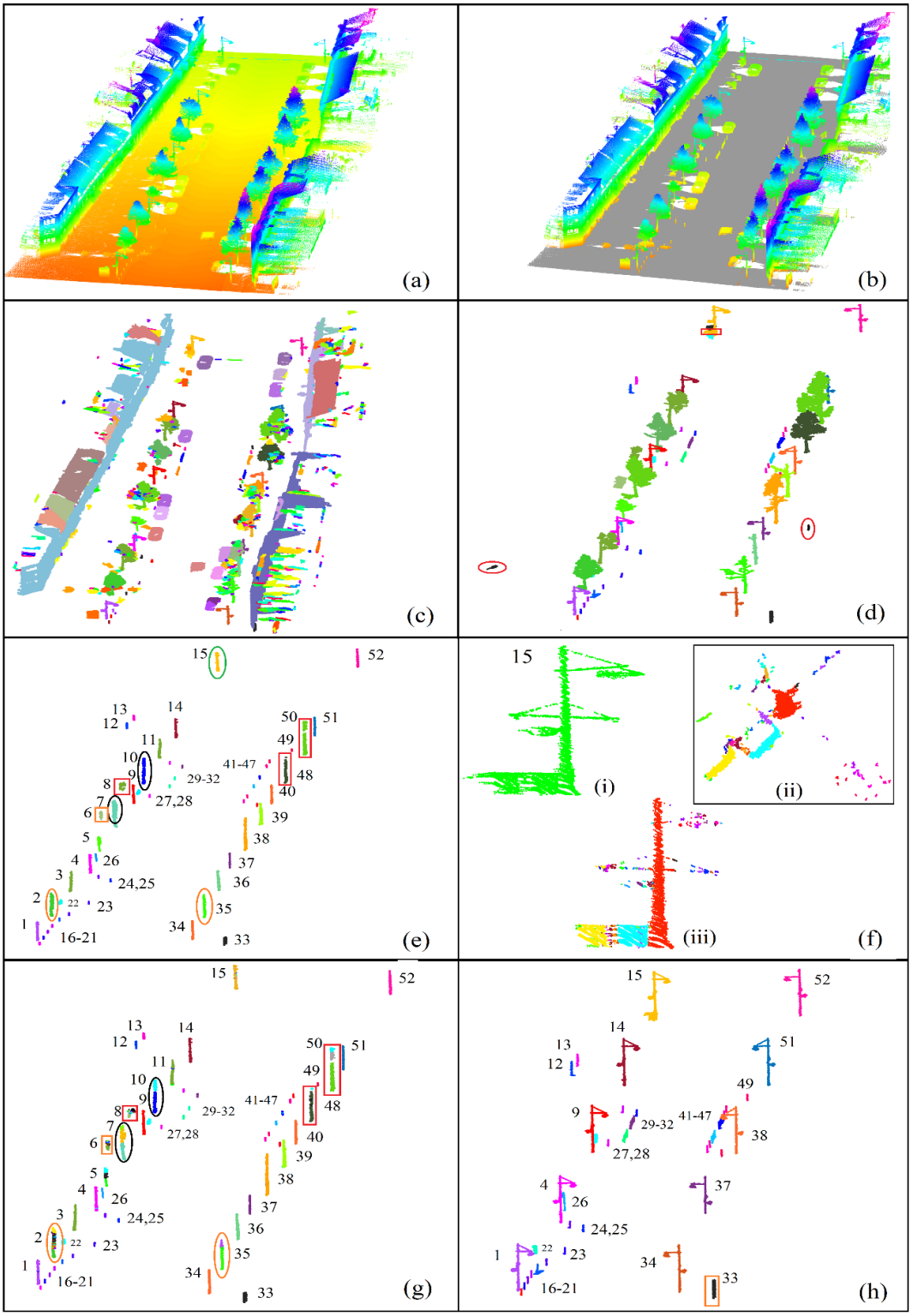

Figure 6. Pole-like objects (PLOs) extraction: (a) MLS point cloud of a road scene, a part of Paris-Lille-3D data, (b) classification of ground and non-ground points, (c) results of spatial clustering, (d) potential PLOs, (e) DBSCAN results, vertical parts detection, (f) DBSCAN result for object 15: (i) a 3D street light pole, (ii) 2D projection results, (iii) detected 3D parts, segments are in different colors, the main vertical part is in red, (g) RD-PCA based segmentation results, (h) results after non-PLOs elimination, extracted PLOs.

https://doi.org/10.5194/isprs-archives-XLVIII-1-W2-2023-27-2023

The selected portion of data covers around 98m of road, has 5,893,301 points, and includes 38 PLOs (i.e., 10 street-light poles, 1 sign pole, 2 circular garbage bins, 4 traffic barriers, 18 bollards, 3 poles attached with roadside building facades) and non-PLOs such as cars, 14 trees, and parts of building facades. The DL method for ground point removal eliminated 3,466,844 points (Fig. 6b). The results of the ED-based spatial clustering on the non-ground points are shown in Fig. 6c. They include a range of whole and partial objects (e.g., facades, trees) with 52 potential PLOs, including 14 trees (Fig 6d). Fig. 6(e) shows the data after the DBSCAN clustering was applied to get the vertical portion of the potential PLOs. Fig. 6(f) shows a close up of some of the DBSCAN results for a street-light pole [object 15, plot (i)]. The 2D and 3D clusters are seen in 6f(ii) and 6f(iii), respectively. The RD-PCA based segmentation on the vertical parts is illustrated in Fig. 6(g). Fig. 6(g) shows that many of the vertical parts from DBSCAN now make more segments due to the unwanted parts that were initially included (mostly from trees). For the RD-PCA based additional segmentation results, the linearity, planarity and scatteredness are verified. Ultimately all trees were successfully removed (e.g., objects 2, 7, 10, 48 and 50). Finally, we extracted all 38 PLOs (Fig, 6h). Objects 12, 13 and 32 in Fig. 6(h) are the three poles that are attached to surrounding building facades.

Non-ground objects		DBSCAN clusters	RD-PCA segments	Extracted PLOs
Street-light pole	10	10	10	10
Sign pole	1	1	1	1
Circular bin	2	2	2	2
Traffic barrier	4	4	4	4
Bollard	18	18	18	18
Pole	3	3	3	3
Tree	14	14	14+15	-
Total	52	52	67	38

Table 1. Distribution of results from different steps.

5. CONCLUSIONS

This paper introduces a robust algorithm for PLOs extraction. First, we removed the ground points using a feature-based DL algorithm that reduces data volume, as well as a computational burden. By coupling the DBSCAN clustering algorithm and the RD-PCA based robust segmentation approach a robust solution is introduced that deals well noise and outliers. The use of DBSCAN in 2D and applied in 3D enabled overcoming initial errors in clustering and successfully identified vertical parts of the potential PLOs. The RD-PCA based segmentation was employed to extract the vertical parts and reduced the influence of outliers/noise on the local saliency feature (e.g., normals) and avoided over and under segmentation errors. The robust normals' z components (Nz) were used to generate a diffusion measure to determine PLOs versus non-PLOs.

The new method was successful for PLOs extraction from a wide variety of urban objects appearing along streets (e.g., street-light poles, utility poles, sign poles, traffic-light signals, billboards, and bollards) taken from two different real-world datasets. The experimental results show that the algorithm has high potential for tree trunk modeling, as well as highway asset health monitoring and additional road object classification. However, the new algorithm is semi-automatic and requires a clear understanding about the underlying data structure to select the necessary parameters used in saliency features estimation and to perform the segmentation tasks. Benchmarking of this work against existing approaches will be the subject of upcoming research.

ACKNOWLEDGEMENTS

Abdul Nurunnabi is funded through the IAS-AUDACITY-PIONEER-2022 project at the University of Luxembourg. A part of this work was developed when Dr Nurunnabi was a postdoctoral scholar at the University of Tokyo.

REFERENCES

Axelsson, P., 2000. DEM generation from laser scanner data using adaptive TIN models. *Int. Arch. Photogramm. Remote Sens. Spat. Inf. Sci*, 33(B4/1), 110–117.

Breiman, L., 2001. Random forests. *Mach. Learn.*, 45(1) : 5–32.

Cabo C., Ordoñez, C., García-Cortés, S., Martínez. J., 2014. An algorithm for automatic detection of pole-like street furniture objects from mobile laser scanner point clouds. *ISPRS J. Photogramm. Remote Sens*., 87 : 47–56.

Chen, Z., Deng, L., Luo, Y., Li, D., et al., 2022. Road extraction in remote sensing data: A survey. *Int. J. Appl. Earth Obs. Geoinf.*, 112: 102833.

Cortes, C., Vapnik, V., 1995. Support-vector networks. *Mach. Learn.*, 20: 273–297.

Ester, M., Kriegel, H-P., Sander, J., Xu. X., 1996. A density-based algorithm for discovering clusters in large spatial databases with noise. *Proc. of the KDD*, AAAI Press, 96(34): 226–231.

Fischler, M.A., Bolles, R.C., 1981. Random sample consensus: a paradigm for model fitting with applications to image analysis and automated cartography. *Commun. ACM*, 24(6): 381–395.

Fang, L., You, Z., Shen, G., Chen, Y., Li, J., 2022. A joint deep learning network of point clouds and multiple views for roadside object classification from lidar point clouds. *ISPRS J. Photogramm. Remote Sens*., 193:115–136.

Golovinskiy, A., Kim, V.G., Funkhouser, T., 2009. Shape-based recognition of 3D point clouds in urban environments. *IEEE ICCV*, 2154–2161.

Ha, T. T., Chaisomphob, T., 2020. Automated localization and classification of expressway pole-like road facilities from mobile laser scanning data. *Adv. Civ. Eng.*, 1–18.

Hubert, M., Rousseeuw, P.J., Branden, K.V., 2005. ROBPCA: a new approach to robust principal component analysis. *Technometrics*, 47(1): 64–79.

Kraus, K., Pfeifer, N., 1998. Determination of terrain models in wooded areas with airborne laser scanner data. *ISPRS J. Photogramm. Remote Sens*., 53(4): 193–203.

Lalonde, J., Vandapel, N., Hebert, M., 2006. Automatic three–dimensional point cloud processing for forest inventory. *CMU-RI-TR-06-21*, The Robot. Inst. CMU, Pennsylvania, USA.

Lehtomäki, M., Jaakkola, A., Hyyppä, J., Lampinen, J., Kaartinen, H., Kukko, A., Puttonen, E., Hyyppä, H., 2015. Object classification and recognition from mobile laser scanning point clouds in a road environment. *IEEE Trans. Geosci. Remote Sens*., 54(2): 1226–1239.

Li, J., Cheng, X., 2022. Supervoxel-based extraction and classification of pole-like objects from MLS point cloud data. *Opt. Laser Technol.*, 146 : 107562.

Liu, R., Wang, P., Yan, Z., Lu, X., Wang, M., Yu, J., et al., 2020. Hierarchical classification of pole-like objects in mobile laser scanning point clouds. *Photogramm. Rec.*, 35(169): 81–107.

Liang, X., Litkey, P., Hyyppa, J., Kaartinen, H., Vastaranta, M., Holopainen, M., 2012. Automatic stem mapping using single-scan terrestrial laser scanning. *IEEE Trans. Geosci. Remote Sens*., 50(2): 661–670.

Luo, D.A., Wang, Y.M., 2008. Rapid extracting pillars by slicing point clouds. *Int. Arch. Photogramm. Remote Sens. Spat. Inf. Sci*, 37: 215–218.

Mitra, N.J., Nguyen, A., 2003. Estimating surface normals in noisy point cloud data. *Proc. of the 19th annual symposium on computational geometry*, 322–328.

Nurunnabi, A., Belton, D., West. G., 2012. Diagnostic-robust statistical analysis for local surface fitting in 3D point cloud data. *ISPRS Annals of the Photogramm. Remote Sens. and Spat. Info. Sci*., 1–3.

Nurunnabi, A., Belton, D., West, G., 2013. Diagnostics based principal component analysis for robust plane fitting in laser data. *16th IEEE International Conference on Computer and Information Technology* (ICCIT), Khulna, Bangladesh. 484–489.

Nurunnabi, A., Hadi, A., Imon, R., 2014a. Procedures for the identification of multiple influential observations in linear regression. *J. Appl. Stat.*, 41 (6), 1315–1331.

Nurunnabi, A., Belton, D., West, G., 2014b. Robust statistical approaches for local planar surface fitting in 3D laser scanning data. *ISPRS J. Photogramm. Remote Sens*., 96: 106–122.

Nurunnabi, A., West, G., Belton, D., 2015. Outlier detection and robust normal-curvature estimation in mobile laser scanning 3D point cloud data. *Pattern Recognit*., 48: 1404–1419.

Nurunnabi, A., West, G., Belton, D., 2016a. Robust locally weighted regression techniques for ground surface points filtering in mobile laser scanning three-dimensional point cloud data. *IEEE Trans. Geosci. Remote Sens*., 54(4): 2181–2193.

Nurunnabi, A., Belton, D., West, G., 2016b. Robust segmentation for large volumes of laser scanning three-dimensional point cloud data. *IEEE Trans. Geosci. Remote Sens*., 54(8): 4790–4805.

Nurunnabi, A., Sadahiro, Y., Lindenbergh, R., Belton, D., 2019. Robust cylinder fitting in laser scanning point cloud data. *Measurement*, 138: 632–651.

Nurunnabi, A., Teferle, N., Li, J., Lindenbergh, R., Hunegnaw, A., 2021. An efficient deep learning approach for ground point filtering in aerial laser scanning point clouds. *Int. Arch. Photogramm. Remote Sens. Spat. Inf. Sci*, XLIII-B1, 31–38.

Nurunnabi, A., Teferle, N., Lindenbergh, R., Li, J., Zlatanova, S., 2022. Robust approach for urban road surface extraction using mobile laser scanning 3D point clouds. *Int. Arch. Photogramm. Remote Sens. Spat. Inf. Sci*, XLIII-B1: 59–66.

Plachetka, C., Fricke,J., Klingner, M., Fingscheidt, T., 2021. DNN-based recognition of pole-like objects in LiDAR point clouds. *Int. Intell. Transp. Syst. Conf.*, Indianapolis, USA, 2889–2896.

Qi, C. R., Su, H., Mo, K., Guibas, L. J., 2017. PointNet: Deep learning on point sets for 3d classification and segmentation. *IEEE CVPR*, 652–660.

Roynard, X., Deschaud, J-E, Goulette, F., 2018. Paris-Lille-3D: A large and high-quality ground-truth urban point cloud dataset for automatic segmentation and classification. *Int J Rob Res*, 37(6): 545–557.

Sheweta, Y., Hussein, A., 2022. Detection of vertical poles in a road environment using monocular images based on YOLOv4. *IEEE Int. Conf. on Vehicular Electronics and Safety*, 1–6.

Sotoodeh, S., 2006. Outlier detection in laser scanner point clouds. *Int. Arch. Photogramm. Remote Sens. Spat. Inf. Sci*., 36(5): 297–302.

Tang, Y., Xiang, Z., Jiang, T., 2020. Semantic classification of pole-like traffic facilities in complex road scenes based on LiDAR point cloud. *Tropical Geography*, 40(5): 893–902.

Tarsha-Kurdi, F., Landes, T., Grussenmeyer, P., 2008. Extended RANSAC algorithm for automatic detection of building roof planes from lidar data. *The photogrammetric journal of Finland*, 21 (1): 97–109.

Tombari, F., Fioraio, N., Cavallari, T., Salti, S., Petrelli, A., Di Stefano, L., 2014. Automatic detection of pole-like structures in 3D urban environments. *IEEE Int. Conf. Intell. Robots Syst.*, 4922–4929.

Vosselman, G., 2000. Slope based filtering of laser altimetry data. *Int. Arch. Photogramm. Remote Sens. Spat. Inf. Sci*, 33(B3/2; PART 3): 935–942.

Wang, Z., Yang, L., Sheng, Y., Shen, M., 2021. Pole-like objects segmentation and multiscale classification-based fusion from mobile point clouds in road scenes. *Remote Sens.*, 13(21): 4382.

Yadav, M., Khan, P., Singh, A. K., 2022. Identification of pole-like objects from mobile laser scanning data of urban roadway scene. *Remote Sensing Applications: Society and Environment*, 26: 100765.

Yu, Y., Li, J., Guan, H., Wang, C., Yu, J., 2015. Semiautomated extraction of street light poles from mobile LiDAR point-clouds. *IEEE Trans. Geosci. Remote Sens*., 53(3): 1374–1386.

Zhang, W., Witharana, C., Li, W., Zhang, C., Li, X, Parent, J., 2018. Using deep learning to identify utility poles with crossarms and estimate their locations from Google Street view images. *Sensors*, 18(8): 2484.